

Low-temperature Hall effect and martensitic transition temperatures in magnetocaloric $\text{Ni}_{50}\text{Mn}_{35}\text{Sb}_{15-x}\text{Ge}_x$ ($x = 0, 1, 3$) alloys

V. V. Marchenkov^{1, 2} and S. M. Emelyanova¹

¹*M. N. Mikheev Institute of Metal Physics of the Ural Branch of the Russian Academy of Science
Ekaterinburg 620108, Russia*

²*Ural Federal University, Ekaterinburg 620002, Russia*

E-mail: march@imp.uran.ru

emelyanova@imp.uran.ru

Received September 23, 2020, published online November 24, 2020

The field dependence of Hall resistivity ρ_H and magnetization M of the magnetocaloric $\text{Ni}_{50}\text{Mn}_{35}\text{Sb}_{15-x}\text{Ge}_x$ ($x = 0, 1, 3$) alloys were measured at $T = 4.2$ K and in magnetic fields of up to 70 kOe. The martensitic transition temperatures, i.e., the martensite start temperature M_S , martensite finish temperature M_F , austenite start A_S and austenite finish A_F temperatures, were obtained from the magnetization temperature dependence that measured from 4.2 to 350 K in a field of 1 kOe. It was observed that the martensitic transition temperatures correlate strongly both with the valence electron concentration e/a and with the electronic transport characteristics, which are the coefficients of normal R_0 and anomalous R_S Hall effect and the concentration of charge carriers n . Apparently, similar correlations should be observed in other magnetocaloric compounds that could be used to study martensitic transitions.

Keywords: magnetocaloric Heusler alloys, Hall effect, normal and anomalous Hall coefficients, valence electron concentration, concentration of charge carriers.

Introduction

The development and synthesis of new Heusler alloys and study of their physical properties are of great fundamental and practical interest since most of them have quite useful functional properties (see, for example, [1, 2] and references therein). A number of Heusler compounds exhibit the shape memory effect [3], the properties of half-metal ferromagnets (HFM) [4–7], spin gapless semiconductors [8–11], topological materials [12], unusual thermal [13] and semiconducting [14–16] properties, *etc.* Heusler alloys with large magnetocaloric effect (MCE) [17–18] are of particular interest because they can be used as a working body in solid-state magnetic refrigerators [19–22]. Traditionally the pure gadolinium or its compounds [for example, silicide-germanide gadolinium $\text{Gd}_5(\text{Si}_2\text{Ge}_2)$] were considered as such materials [23].

Heusler alloys based on the systems of Ni–Mn–X ($X = \text{Ga}, \text{In}, \text{Sb}, \text{Sn}$) recently have become increasingly an alternative, since these alloys can exceed the compounds with gadolinium in the value of MCE for the magnetic field of the same magnitude [24]. The giant values of the MCE

are achieved in them due to the structural transformation accompanying the magnetic transition. In addition, various single- or multi-layered structures are also considered for use in magnetic cooling technology [25, 26].

The e/a ratio (the number of valence electrons per atom) is one of the main parameters, which correlates with the martensitic transition temperatures (MTT). In this case the direct relationship between e/a and MTT is observed, i.e., the MTT increase when the e/a ratio grows. However, these trends are not always traced. It was reported about non-monotonic dependence of M_S on e/a in $\text{Ni}_{50}\text{Mn}_{35-x}\text{Cu}_x\text{Sn}$ [27] and $\text{Ni}_{2-x}\text{Cu}_x\text{MnGa}$ [28] compounds. In particular, in Ref. 29 it is indicated that the e/a ratio in $\text{Ni}_{48}\text{Mn}_{39}\text{Sn}_{13-x}\text{Si}_x$ ($1 \leq x \leq 4$) system alloys does not change with an increase in the Si content and is constantly equal to 8.05, however, the M_S temperature decreases. In addition, for the Ni–Mn–Ga [30] and Ni–Mn–In–Sb systems [31], it was found that the MTT decreases even if the substitution leads to an increase in the e/a ratio. Moreover, in Ref. 32 it was shown that the e/a ratio is insufficient to describe the behavior of MTT in four-component Heusler-like alloys.

In Ref. 33 it was demonstrated that the MTT for the alloys $\text{Ni}_{44}\text{Mn}_{45}\text{Sn}_{10}\text{R}$ ($\text{R} = \text{Al}, \text{Ga}, \text{In}, \text{and Sn}$) increase monotonously with the increasing of electron density, which is proportional to the e/a ratio divided by the cell volume V_{cell} of austenite. In addition, it is indicated that the parameters of the crystal lattice and, consequently, the V_{cell} for the same compound can significantly vary depending on the alloy preparation method.

In Ref. 34, at studying the Ni–Mn–In alloys, it was proposed to use the Hall coefficients and the concentration of charge carriers n as the electronic parameters characterizing the MTT. It was suggested [34] that a similar relationship can be observed in other magnetocaloric alloys. In particular, such correlation can be realized in Ni–Mn–Sb alloys since the martensitic transformations in these compounds occur. That is why the Ni–Mn–Sb Heusler-like alloys were chosen as the objects. The purpose of this work is to search for and study the correlation between the electronic characteristics, namely, the Hall coefficients, the concentration of charge carriers, and the e/a ratio with the MTT, in the magnetocaloric $\text{Ni}_{50}\text{Mn}_{35}\text{Sb}_{15-x}\text{Ge}_x$ ($x = 0, 1, 3$) alloys.

2. Experimental

The $\text{Ni}_{50}\text{Mn}_{35}\text{Sb}_{15-x}\text{Ge}_x$ ($x = 0, 1, 3$) ingots were prepared by arc melting in an inert atmosphere and subsequently subjected to annealing at 1100 K for 24 h followed by furnace cooling. The samples for Hall effect and magnetization measurements were cut from preparing ingots by spark cutting. The elemental analysis was performed using an Inspect F scanning electron microscope (FEI Company, USA) equipped with a field-emission cathode and an EDAX spectrometer. The examination showed that the deviation from the stoichiometric composition were insignificant in all alloys (Table 1). The structural analysis was performed at the Collaborative Access Center «Testing Center of Nanotechnology and Advanced Materials» of the Institute of Metal Physics, UB RAS.

Table 1. Chemical composition in the $\text{Ni}_{50}\text{Mn}_{35}\text{Sb}_{15-x}\text{Ge}_x$ ($x = 0, 1, 3$) alloys, at. %

Alloy	Ni	Mn	Sb	Ge
$\text{Ni}_{50}\text{Mn}_{35}\text{Sb}_{15}$	49.9	35.4	14.7	–
$\text{Ni}_{50}\text{Mn}_{35}\text{Sb}_{14}\text{Ge}_1$	49.7	35.4	13.7	1.2
$\text{Ni}_{50}\text{Mn}_{35}\text{Sb}_{12}\text{Ge}_3$	49.7	35.5	11.7	3.1

X-ray diffraction patterns were taken at room temperature in an angular range of 5° – 120° . XRD analysis indicated that all investigated alloys possess $L2_1$ -structure.

The magnetic and galvanomagnetic properties were measured at MPMS XL7 SQUID magnetometer and PPMS setup (Quantum Design). The magnetic properties were measured in magnetic fields of up to 70 kOe in the temperatures range from 4.2 to 350 K. The Hall effect was measured by the standard dc four-probe method at temperature 4.2 K and in magnetic fields of up to 100 kOe. The copper

wire leads were spot-welded to the samples. The Hall resistivity was determined by four measurements performed by switching an electric current and a magnetic field [35]. For a uniform current distribution, the ratio of the sample sizes for Hall effect measurements must satisfy 1 : 3 : 9, our samples were the plates of $0.5 \times 1.5 \times 4.5$ mm in size, hence, the demagnetization factor $N = 1$ for such samples. A magnetic field vector was normal to the plate plane accurate within $\pm 2^\circ$ (or $\pm 2.5\%$), and an electric current passed along the largest sample face.

3. Results and discussion

As an example Fig. 1 shows the temperature dependence of magnetization for the alloy $\text{Ni}_{50}\text{Mn}_{35}\text{Sb}_{15}$ which was measured upon cooling and heating (shown by arrows) in a magnetic field $H = 1$ kOe. The form of this dependences is typical for all investigated alloys. It can be seen that the $M(T)$ curves exhibit minima and maxima, as well as hysteresis in the region of MTT (A_S, A_F, M_S, M_F).

The MTT were determined from the temperature dependences of the magnetization and electrical resistance using the method of tangents [36 and references therein, 37], according to which this temperatures were determined at their intersection (Table 2). It can be seen (Table 2) that the values of MTT, determined from the experiment, are agreed well with the literature data for these alloys [38, 39]. A decrease in MTT with an increase in the germanium content is observed, i.e., with a decrease in the e/a ratio.

The calculation of e/a ratio was carried out according to the Eq. (1) below [36 and references therein] as the sum of the products of the number of valence d - and s -electrons of the chemical element including in the alloy, on the fraction of this chemical element:

$$\frac{e}{a} = (C_A \cdot Z_A) + (C_B \cdot Z_B) + (C_D \cdot Z_D), \quad (1)$$

where C_A, C_B, C_D are the concentrations of A-, B- and D-elements; Z_A, Z_B, Z_D are the number of external (valence)

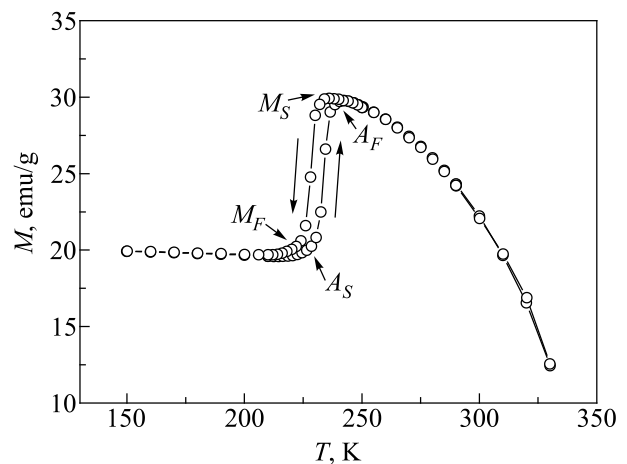


Fig. 1. Temperature dependences of magnetization for the alloys $\text{Ni}_{50}\text{Mn}_{35}\text{Sb}_{15}$ in a magnetic field $H = 1$ kOe.

Table 2. Martensitic transition temperatures, e/a ratio, normal R_0 and anomalous R_S Hall effect coefficients and concentration of charge carriers n for the $\text{Ni}_{50}\text{Mn}_{35}\text{Sb}_{15-x}\text{Ge}_x$ ($x = 0, 1, 3$) alloys. The temperatures of the start and finish of martensitic transformation are designated as M_S and M_F respectively; the temperatures of the start and finish of austenitic transformation are A_S and A_F , respectively

Alloy	A_S , K	A_F , K	M_S , K	M_F , K	e/a	R_0 , cm^3/C	R_S , cm^3/C	$n \cdot 10^{22}$, $1/\text{cm}^3$
$\text{Ni}_{50}\text{Mn}_{35}\text{Sb}_{15}$	232	245	230	215	8.20	$-1.2 \cdot 10^{-4}$	0.137	5.33
$\text{Ni}_{50}\text{Mn}_{35}\text{Sb}_{14}\text{Ge}_1$	215	223	212	210	8.19	$-9.9 \cdot 10^{-5}$	0.111	6.28
$\text{Ni}_{50}\text{Mn}_{35}\text{Sb}_{12}\text{Ge}_3$	203	207	195	193	8.17	$-9.4 \cdot 10^{-5}$	0.092	6.64

electrons for the elements of A, B and D. The number of valence electrons was assumed to be 10, 7, 5 and 4 for Ni ($3d^8 4s^2$), Mn ($3d^6 4s^1$), Sb ($5s^2 5p^3$) and Ge ($4s^2 4p^2$), respectively.

In Ref. 38, where the MCE of the $\text{Ni}_{50}\text{Mn}_{35}\text{Sb}_{15-x}\text{Z}_x$ ($Z = \text{Al, Ge}; x = 0, 2$) alloys was studied, it was suggested that one of the possible reason for significant change of the MTT could be a change in the density of electronic states at the Fermi level E_F and/or a shift in E_F with a change in the composition alloys. In this case, changes not only in the electrical resistivity should be observed, but in other electronic transport properties as well, in particular, in the galvanomagnetic properties, for example in the Hall effect. Since at low temperatures the $\text{Ni}_{50}\text{Mn}_{35}\text{Sb}_{15-x}\text{Ge}_x$ ($x = 0, 1, 3$)

alloys are in a ferromagnetic state (FM), than at $T = 4.2$ K in addition to the normal Hall effect, the anomalous one should be observed also. Since for the separation of the normal and anomalous components of the Hall effect the data on magnetization are required, in addition to the field dependences of the Hall resistivity $\rho_H(H)$ [Fig. 2(a)], the field dependences of the magnetization $M(H)$ [Fig. 2(b)] were also measured.

The field dependences of the Hall resistivity $\rho_H(H)$ and the magnetization curves at 4.2 K have the same general view. The curves $\rho_H(H)$ and $M(H)$ have two distinguishable intervals of magnetic fields, such as the technical magnetization region ($H < 10$ kOe), and the paraprocess region at higher fields. Figure 2 shows that in the region of technical magnetization for both $\rho_H(H)$ and $M(H)$ a sharp increase with increasing the magnetic field is observed.

Taking into account the fact that for $\rho_H(H)$ and $M(H)$ curves there is no saturation effect and no linear dependence even in high magnetic fields, we used the approach proposed in Ref. 40. The coefficients of normal R_0 and anomalous R_S Hall effect were determined from the dependences of $\rho_H(H)$ and $M(H)$ in the paraprocess region using the following equation:

$$\frac{\rho_H}{H} = R_0 + \frac{4\pi R_S^* M}{H}, \quad (2)$$

where $R_S^* = R_S + (1 - N)R_0$, N is the demagnetization factor, which equals 1 for samples studied, hence, $R_S^* \approx R_S$ in our case. The first term in Eq. (2) describes the normal Hall effect (NHE), which is caused by the Lorentz force on the charge carriers and is proportional to the applied magnetic field. The second term in Eq. (2) is determined by so-called anomalous Hall effect (AHE).

From Fig. 3 it can be seen that the Eq. (2) is valid for all investigated alloys in the region of high magnetic fields ($H > 20$ kOe). Using the experimental data (Fig. 3) and Eq. (2), the NHE R_0 and AHE R_S coefficients were obtained (see Table 2 and Fig. 4).

Figure 4 shows the dependences of the NHE and AHE coefficients on the e/a ratio for all the studied alloys. It can be seen [Fig. 4(a)] that the NHE coefficient is negative, i.e., the main type of charge carriers are electrons, and its value decreases with the growth of the e/a ratio. The AHE is positive, and in absolute value it is 3 orders of magnitude higher than the NHE values [Fig. 4(b)]. At the same time, the AHE

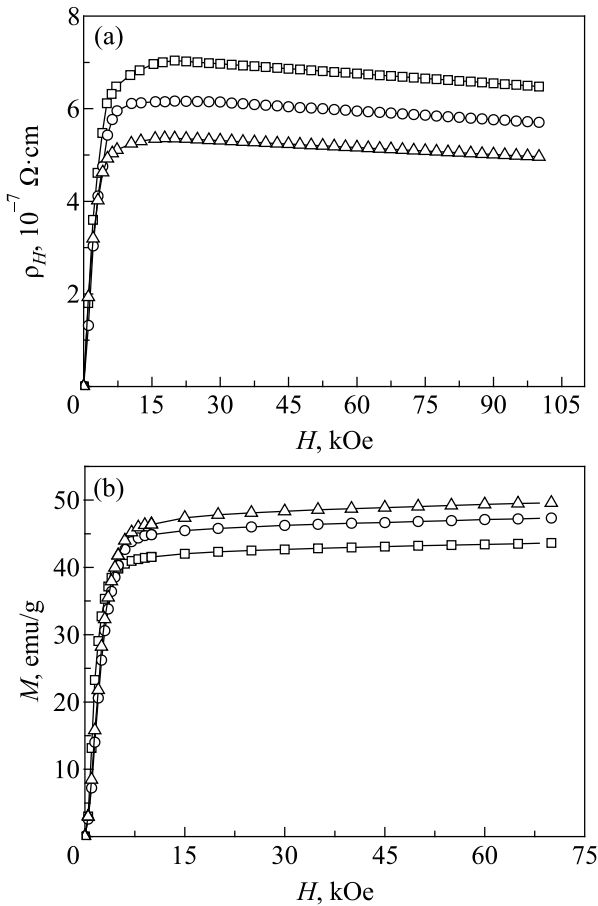


Fig. 2. Field dependences of the Hall resistivity $\rho_H(H)$ at $T = 4.2$ K (a) and field dependences of magnetization $M(H)$ at $T = 4.2$ K (b): $\text{Ni}_{50}\text{Mn}_{35}\text{Sb}_{15}$ (\square), $\text{Ni}_{50}\text{Mn}_{35}\text{Sb}_{14}\text{Ge}_1$ (\circ), $\text{Ni}_{50}\text{Mn}_{35}\text{Sb}_{12}\text{Ge}_3$ (\triangle).

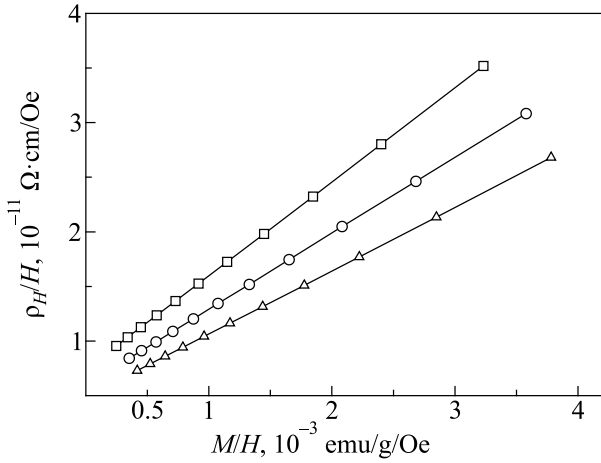


Fig. 3. Dependences ρ_H/H on M/H for $\text{Ni}_{50}\text{Mn}_{35}\text{Sb}_{15-x}\text{Ge}_x$ ($x = 0, 1, 3$) alloys at $T = 4.2$ K: $\text{Ni}_{50}\text{Mn}_{35}\text{Sb}_{15}$ (\square), $\text{Ni}_{50}\text{Mn}_{35}\text{Sb}_{14}\text{Ge}_1$ (\circ), $\text{Ni}_{50}\text{Mn}_{35}\text{Sb}_{12}\text{Ge}_3$ (\triangle).

monotonically changes as well with the change in the e/a ratio, but unlike the NHE, the AHE increases with the growth of e/a ratio. These results are in qualitative agreement with the results of [34], where the Hall effect in magnetocaloric alloys of the Ni–Mn–In system is studied.

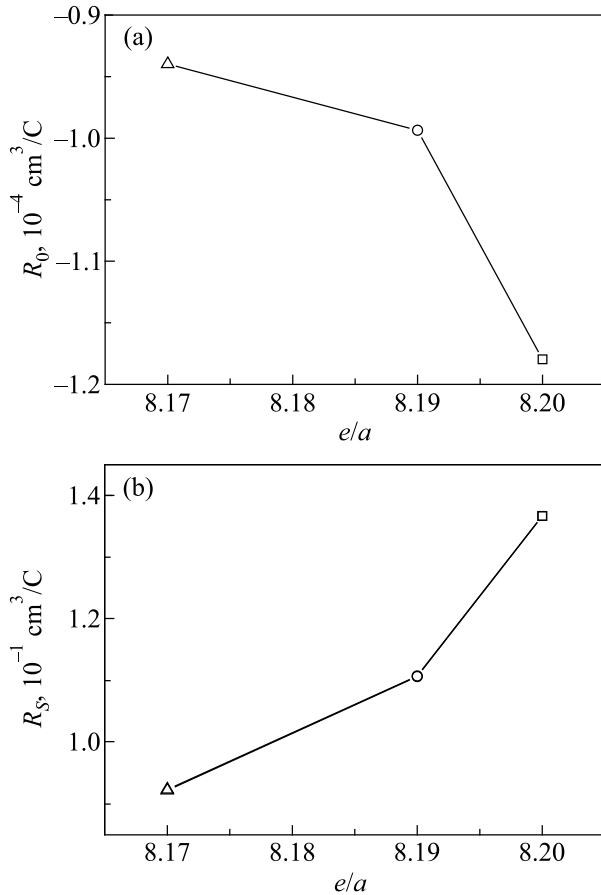


Fig. 4. Dependences of the normal R_0 (a) and anomalous R_S (b) Hall coefficients on the e/a ratio: $\text{Ni}_{50}\text{Mn}_{35}\text{Sb}_{15}$ (\square), $\text{Ni}_{50}\text{Mn}_{35}\text{Sb}_{14}\text{Ge}_1$ (\circ), $\text{Ni}_{50}\text{Mn}_{35}\text{Sb}_{12}\text{Ge}_3$ (\triangle).

The NHE coefficient R_0 is characterized by the number n of current carriers per unit specimen volume using the following equation:

$$R_0 = \frac{1}{nec}, \quad (3)$$

where c is the light velocity, e is the charge of electron.

It should be noted that the Fermi surface of Heusler alloys has a complex topology and contains the various sheets of both electronic and hole types. Therefore, to accurately determine the concentration of charge carriers, it is necessary to have the data on Fermi surface topology of certain alloy, as well as the data on the mobility of charge carriers belonging to certain sheets of the Fermi surface. This is quite a challenge. However, as shown in [10, 11, 41, 42], estimating the concentration of charge carriers using one band model makes it possible to qualitatively track the changes in the electronic characteristics and qualitatively determine the correlation between them even in such complex compounds. Therefore, we use one band model likewise [43].

Using a one band model and the obtained experimental data, the values of charge carrier concentration were estimated (Table 2 and Fig. 5). As already noted, the main type of charge carriers are electrons, and their concentration increases with an increase in the e/a ratio (Table 2). Figure 5 demonstrates a correlation between MTT and the concentration of charge carriers as well, i.e., the values of MTT monotonically decrease with an increase in the concentration n . A similar relationship was also observed in [34] in the alloys of the Ni–Mn–In system. It seems that an analogous relationship between MTT and the concentration of charge carriers can be observed in other magnetocaloric alloys. In addition, a similar correlation may exist between the MTT and other parameters of the electronic subsystem of such MCE compounds.

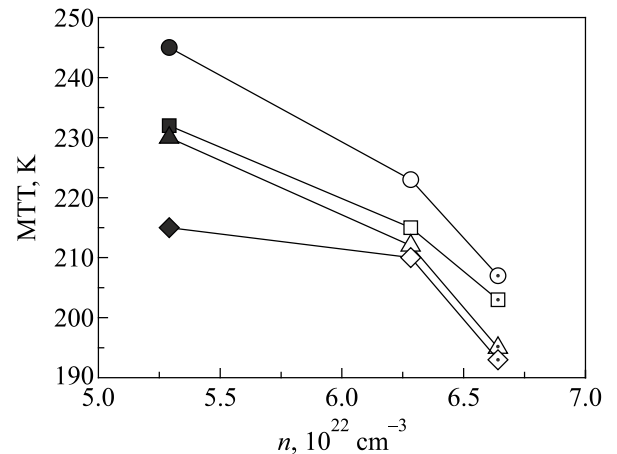


Fig. 5. Dependences of the MTT on the concentration of current carriers: filled symbols — $\text{Ni}_{50}\text{Mn}_{35}\text{Sb}_{15}$, open symbols — $\text{Ni}_{50}\text{Mn}_{35}\text{Sb}_{14}\text{Ge}_1$, symbols with point — $\text{Ni}_{50}\text{Mn}_{35}\text{Sb}_{12}\text{Ge}_3$; squares — A_S , circles — A_F , triangles — M_S , rhombuses — M_F .

It should be noted that in this paper, the low-temperature Hall effect was studied at $T = 4.2$ K, while the values of MTT refer to higher temperatures. Apparently, the Hall effect, as well as other electronic transport properties should be investigated at temperatures comparable with MTT in order to determine the parameters of the electronic subsystem and compare them with MTT. However, in this paper, as in [34], a correlation between MTT and concentration of charge carriers n was demonstrated, which, apparently, can be used for study the relationship between the electronic and thermodynamic characteristics of MCE-systems, in particular, MCE Heusler alloys.

Conclusions

Thus, as a result of studying the low-temperature Hall effect and the magnetization of $\text{Ni}_{50}\text{Mn}_{35}\text{Sb}_{15-x}\text{Ge}_x$ ($x = 0, 1, 3$) magnetocaloric alloys, the following conclusions can be drawn. A relationship was established between the Hall effect and the e/a ratio, i.e., the NHR R_0 decreases and the AHE R_S increases with the growth of e/a ratio. A correlation between the concentration of charge carriers n and the MTT (A_S , A_F , M_S , and M_F) was found, namely, MTT monotonically decrease with increasing n . It is suggested that a similar relationship should exist in other MCE Heusler alloys, and the obtained results can be used to study the relationship between the electronic and thermodynamic parameters of such systems.

Acknowledgements

This work was partly supported by the state assignment of Ministry of High Education and Science of Russia (theme "Spin" No. AAAA-A18-118020290104-2), by the RFBR (project No. 18-02-00739) and by the Government of the Russian Federation (decision No. 211, contract No. 02.A03.21.0006).

1. T. Graf, C. Felser, and S. S. P. Parkin, *Prog. Solid. State. Chem.* **39**, 1 (2011).
2. L. Wollmann, A. K. Nayak, S. S. P. Parkin, and C. Felser, *Annu. Rev. Mater. Res.* **47**, 247 (2017).
3. A. N. Vasiliev, V. D. Buchelnikov, T. Takagi, V. V. Khovailo, and E. I. Estrin, *UFN* **173**, 577 (2003).
4. M. I. Katsnelson, V. Yu. Irkhin, L. Chioncel, A. I. Lichtenstein, and R. A. de Groot, *Rev. Mod. Phys.* **80**, 315 (2008).
5. N. I. Kourov, V. V. Marchenkov, A. V. Korolev, K. A. Belozerova, and H. W. Weber, *Curr. Appl. Phys.* **15**, 839 (2015).
6. N. I. Kourov, V. V. Marchenkov, A. V. Korolev, L. A. Stashkova, S. M. Emelyanova, and H. W. Weber, *Phys. Solid State* **57**, 700 (2015).
7. Yu. A. Perevozchikova, A. A. Semiannikova, A. N. Domozhirova, P. B. Terentev, E. B. Marchenkova, E. I. Patrakov, M. Eisterer, P. S. Korenistov, and V. V. Marchenkov, *Fiz. Nizk. Temp.* **45**, 921 (2019) [*Low Temp. Phys.* **45**, 789 (2019)].
8. X. L. Wang, *Phys. Rev. Lett.* **100**, 156404 (2008).
9. S. Ouardi, G. H. Fecher, and C. Felser, *Phys. Rev. Lett.* **110**, 100401 (2013).
10. V. V. Marchenkov, V. Yu. Irkhin, Yu. A. Perevozchikova, P. B. Terent'ev, A. A. Semiannikova, E. B. Marchenkova, and M. Eisterer, *JETP* **128**, 919 (2019).
11. V. V. Marchenkov, N. I. Kourov, and V. Yu. Irkhin, *Phys. Met. Metallog.* **119**, 1321 (2018).
12. K. Manna, Y. Sun, L. Muechler, J. Kübler, and C. Felser, *Nat. Rev. Mater.* **3**, 244 (2018).
13. S. M. Podgornykh, A. D. Svyazhin, E. I. Schreder, V. V. Marchenkov, and V. P. Dyakina, *JETP* **105**, 42 (2007).
14. Y. Nishino, M. Kato, S. Asano, K. Soda, M. Hayasaki, and U. Mizutani, *Phys. Rev. Lett.* **79**, 1909 (1997).
15. V. I. Okulov, V. E. Arkhipov, T. E. Govorkova, A. V. Korolev, V. V. Marchenkov, K. A. Okulova, E. I. Schreder, and H. W. Weber, *Fiz. Nizk. Temp.* **33**, 907 (2007) [*Low Temp. Phys.* **33**, 692 (2007)].
16. V. I. Okulov, A. T. Lonchakov, and V. V. Marchenkov, *Phys. Met. Metallog.* **119**, 1325 (2018).
17. H. C. Xuan, Y. Q. Zhang, H. Li, P. D. Han, D. H. Wang, and Y. W. Du, *Phys. Status Solidi A* **212** (3), 680 (2014).
18. P. A. Bhohe, K. R. Priolkar, and A. K. Nigam, *Appl. Phys. Lett.* **91**, 242503 (2007).
19. A. Kitanovski, U. Plaznik, U. Tomc, and A. Poredoš, *Int. J. Refrig.* **57**, 288 (2015).
20. M. I. Pashchenko, V. A. Bedarev, D. N. Merenkov, A. N. Bludov, V. A. Pashchenko, and S. L. Gnatchenko, *Fiz. Nizk. Temp.* **43**, 789 (2017) [*Low Temp. Phys.* **43**, 631 (2017)].
21. E. Zubov, N. Nedelko, A. Sivachenko, K. Dyakonov, Yu. Tyvanchuk, M. Marzec, V. Valkov, W. Bažela, A. Ślowska-Waniewska, V. Dyakonov, A. Szytuła, and H. Szymczak, *Fiz. Nizk. Temp.* **44**, 989 (2018) [*Low Temp. Phys.* **44**, 775 (2018)].
22. V. A. L'vov, A. Kosogor, and V. A. Chernenko, *Fiz. Nizk. Temp.* **46**, 909 (2020) [*Low Temp. Phys.* **46**, 764 (2020)].
23. V. K. Pecharsky and K. A. Gschneidner, *Phys. Rev. Lett.* **78**, 4494 (1997).
24. J. Liu, T. Gottoschall, K. P. Skokov, J. D. Moore, and O. Gutfleisch, *Nat. Mater.* **11**, 620 (2012).
25. J. Tušek, A. Kitanovski, U. Toms, C. Favero, and A. Poredoš, *Int. J. Refrig.* **37**, 117 (2014).
26. K. Navickaitė, H. N. Bez, T. Lei, A. Barcza, H. Vieyra, C. R. H. Bahl, and K. Engelbrecht, *Int. J. Refrig.* **86**, 322 (2018).
27. B. Gao, J. Shen, F. X. Hu, J. Wang, J. R. Sun, and B. G. Shen, *Appl. Phys. A* **97**, 443 (2009).
28. T. Kanomata, T. Nozawa, D. Kikuchi, H. Nishihara, K. Koyama, and K. Watanabe, *Int. J. Appl. Electrom.* **21**, 151 (2005).
29. S. Esakki Muthu, S. Singh, R. Thiyagarajan, G. Kalai Selvan, N. V. Rama Rao, M. Manivel Raja, and S. Arumugam, *J. Phys. D: Appl. Phys.* **46**, 205001 (2013).
30. Z. H. Liu, M. Zhang, W. Q. Wang, W. H. Wang, J. L. Chen, G. H. Wu, F. B. Meng, H. Y. Liu, B. D. Liu, J. P. Qu, and Y. X. Li, *Appl. Phys.* **92**, 5006 (2002).
31. Z. Liu, Z. Wu, H. Yang, Y. Liu, E. Liu, H. Zhang, and G. Wu, *Intermetallics* **18**, 1690 (2010).

32. D. Comtesse, M. E. Gruner, M. Ogura, V. V. Sokolovskiy, V. D. Buchelnikov, A. Grünebohm, R. Arróyave, N. Singh, T. Gottschall, O. Gutfleisch, V. A. Chernenko, F. Albertini, S. Fähler, and P. Entel, *Phys. Rev. B* **89**, 184403 (2014).
33. R. L. Wang, J. B. Yan, H. B. Xiao, L. S. Xu, V. V. Marchenkov, L. F. Xu, and C. P. Yang, *J. Alloys Compd.* **509**, 6834 (2011).
34. V. V. Marchenkov and S. M. Emelyanova, *Submitted to Metals* (2020).
35. N. I. Kourov, V. V. Marchenkov, K. A. Belozeroва, and H. W. Weber, *JETP* **121**, 844 (2015).
36. *Shape Memory Titanium Nickelide Alloys C I Structure, Phase Transformers and Properties*, V. G. Pushin (ed.), Ural Branch of RAS, Ekaterinburg (2006).
37. D. H. Wang, C. L. Zhang, H. C. Xuan, Z. D. Han, J. R. Zhang, S. L. Tang, B. X. Gu, and Y. W. Du, *J. Appl. Phys.* **102**, 013909 (2007).
38. S. M. Emelyanova, N. G. Bebenin, V. P. Dyakina, V. V. Chistyakov, T. V. Dyachkova, A. P. Tyutyunnik, R. L. Wang, C. P. Yang, F. Sauerzopf, and V. V. Marchenkov, *Phys. Met. Metallog.* **119**, 157 (2018).
39. S. Aksoy, M. Acet, E. F. Wassermann, T. Krenke, X. Moya, L. Mañosa, A. Planes, and P. P. Deen, *Phil. Mag.* **89**, 2093 (2009).
40. N. I. Kourov, V. V. Marchenkov, Yu. A. Perevozchikova, and H. W. Weber, *Phys. Solid State* **59**, 63 (2017).
41. N. I. Kourov, V. V. Marchenkov, A. V. Korolev, A. V. Lukoyanov, A. A. Shirokov, and Yu. A. Perevozchikova, *Mater. Res. Express* **4**, 116102 (2017).
42. V. V. Marchenkov, Yu. A. Perevozchikova, N. I. Kourov, V. Yu. Irkhin, M. Eisterer, and T. Gao, *J. Magn. Magn. Mater.* **459**, 211 (2018).
43. I. M. Lifshits, M. Ya. Azbel, and M. I. Kaganov, *Electron Theory of Metals*, Consultants Bureau, New York (1973).

Низькотемпературний ефект Холла та температури мартенситних перетворень у магнітокалоричних сплавах $\text{Ni}_{50}\text{Mn}_{35}\text{Sb}_{15-x}\text{Ge}_x$ ($x = 0, 1, 3$)

V. V. Marchenkov, S. M. Emelyanova

Виміряно польові залежності опору Холла ρ_H та намагніченості M магнітокалоричних сплавів $\text{Ni}_{50}\text{Mn}_{35}\text{Sb}_{15-x}\text{Ge}_x$ ($x = 0, 1, 3$) при $T = 4,2$ К у магнітних полях до 70 кЕ. Температури мартенситних перетворень, тобто температура початку мартенситу M_S , кінця мартенситу M_F , початку аустеніту A_S , кінця аустеніту A_F , отримано із температурної залежності намагнічування, яка вимірювалась від 4,2 К до 350 К у полі 1 кЕ. Виявлено, що температури мартенситних переходів сильно корелюють як із концентрацією валентних електронів e/a , так і з електронними транспортними характеристиками, тобто коефіцієнтами нормального R_0 і аномального R_S ефекту Холла та концентрацією носіїв заряду n . Мабуть, аналогічні кореляції повинні спостерігатися в інших магнітокалоричних сполуках, які можуть бути використані для вивчення мартенситних переходів.

Ключові слова: магнітокалоричні сплави Гейслера, ефект Холла, нормальний та аномальний коефіцієнти Холла, концентрація валентних електронів, концентрація носіїв заряду.